Available online at www.sciencedirect.com

ScienceDirect

Advances in Space Research 68 (2021) 3205–3217

ADVANCES IN SPACE RESEARCH (a COSPAR publication)

www.elsevier.com/locate/asr

Future Venus missions and flybys: A collection of possible measurements with mass spectrometers and plasma instruments

S. Gruchola *, A. Galli, A. Vorburger, P. Wurz

Physikalisches Institut, University of Bern, Sidlerstrasse 5, 3012 Bern, Switzerland

Received 12 February 2021; received in revised form 1 June 2021; accepted 21 July 2021
Available online 30 July 2021

Abstract

This study contains predictions for mass spectrometry and plasma instrument measurements during upcoming Venus flybys of BepiColombo and Solar Orbiter and discusses the possibility of a phosphine detection with mass spectrometry in Venus' upper atmosphere. The results extend the ones published previously in Gruchola et al. (2019), where predictions for the proposed ESA mission EnVision and the Venus flyby of JUICE were included. Both the Venus flyby of BepiColombo and the one of Solar Orbiter will take place in August 2021, only 1 day apart. BepiColombo, carrying the neutral mass gas spectrometer STROFIO, could probe the atmosphere around closest approach and obtain data on the thermal and hot neutral particle populations in the upper atmosphere. According to this study, the thermal hydrogen population as well as the hot species H, C, N and O, including isotopes, should be visible to STROFIO. Especially data on the abundance of the hot species would yield important insight into the planetary escape processes. The Solar Orbiter on the other hand carries the plasma instrument SWA-HIS, designed to measure the energetic solar wind ions. During its second Venus gravity assist it will traverse the magnetosheath, the region between bow shock and ion composition boundary, where in addition to the solar wind ions energetic planetary ions are present. The planetary pickup ions can be measured by SWA-HIS, providing important information on the outflow of planetary ions and the ionization processes in the upper atmosphere itself. The recent reports of phosphine in Venus' cloud decks with an abundance of 20 ppb at 80 km probably overestimate the actual PH_3 abundance, as the data are currently being reanalyzed (Greaves et al., 2021). However, even with this upper limit of 20 ppb a phosphine detection with a mass spectrometer e.g. on-board ESA's proposed EnVision mission, seems unlikely. To resolve the PH_3 peak and the $^{16}O^{18}O$ peak a mass resolution of almost 10'000 is required, and the PH_2D peak is masked by the Cl fragment peak of HCl. Furthermore, NGMS on-board Pioneer Venus with a mass resolution of around 440 did most likely not detect phosphine, as it scanned only a few masses in the mass range of interest where more abundant species than phosphine are present.

Keywords: Venus; Mass spectrometry; BepiColombo; Solar Orbiter; Phosphine

1. Introduction

Venus is our closest planetary neighbor, and several space missions were dedicated to learning more about its composition and chemistry. It all started with the Mariner and Venera missions of the United States and the Soviet Union, respectively, in the sixties (Bailey, 2013). The Venera missions continued well into the eighties and also performed the first successful lander mission (Basilevsky et al., 2007).

In 1978 the Pioneer Venus mission by the United States launched with two separate spacecraft, an orbiter (Pioneer Venus 1) and a multiprobe (Pioneer Venus 2) (Johnson and de Oliveira, 2019). It was designed to study many different aspects of Venus, among which were the clouds, the inter-

* Corresponding author.
E-mail addresses: salome.gruchola@space.unibe.ch (S. Gruchola), andre.galli@space.unibe.ch (A. Galli), audrey.vorburger@space.unibe.ch (A. Vorburger), peter.wurz@space.unibe.ch (P. Wurz).

https://doi.org/10.1016/j.asr.2021.07.024
0273-1177/

action of the solar wind with the ionosphere, the surface, the thermal balance and the atmospheric composition. To measure the latter, the payload included an ion mass spectrometer and neutral mass spectrometer, an ultra-violet spectrometer and a gas chromatograph. The orbiter conducted in situ measurements on the night side above 140 km above the surface, in the so-called exosphere (Kasprzak, 1990). On the day side, the exobase lies significantly higher at around 210 km, it sinks during the night because of IR emissions from the CO_2 atmosphere (Kasprzak et al., 1997). In the exosphere, species tend to separate according to their mass, i.e., the scale height becomes mass dependent. The atmospheric region below 100 km is called homosphere and is well mixed, meaning that when neglecting chemical processes all species have the same scale height and constant mixing ratios within the whole homosphere. The Pioneer Venus orbiter mission hence acquired data in-between the homosphere and the exosphere (Kasprzak, 1990). The multiprobe on the other hand studied the lower atmosphere of Venus from an altitude of 62 km down to the surface (Hoffman et al., 1980).

After Pioneer Venus the Vega and Magellan missions followed, then the ESA mission Venus Express in 2005 and more recently the Japanese mission Akatsuki in 2010, which is still collecting data (Johnson and de Oliveira, 2019). Venus Express studied the atmospheric structure and chemistry, the cloud layers and hazes as well as the atmospheric escape processes. The science payload included the UV-IR spectrometers SPICAV and SOIR, and the UV–vis-IR spectrometer VIRTIS (Svedhem et al., 2009). Another instrument on-board VEX was the plasma instrument ASPERA-4 (Analyzer of Space Plasmas and Energetic Atoms) designed to study the interactions of the solar wind with the atmosphere of Venus and to characterise the plasma and neutral gas environment in the near-Venus space through energetic neutral atom (ENA) imaging and local charged particle measurements. (Barabash et al., 2007).

In addition to the missions mentioned above Venus had also other, shorter visitors. One of them was the Galileo spacecraft, which used Venus for a gravity assist on its way to Jupiter in 1990. It was a good opportunity to check the performance of the scientific instruments on-board. Thus, Galileo looked for impulsive radio signals with its plasma instrument. The signals it measured confirmed that lightning exists on Venus, which was not entirely resolved yet as the data measured by Venera and Pioneer Venus were inconclusive. Lightning represents an important atmospheric process that is indicative of convective storms and can be a sign of active volcanism (Gurnett et al., 1991). More recently, the Venus Monitoring Camera (VMC) on-board VEX provided further evidence for active volcanism by monitoring brightness changes of several locations on the surface of Venus, which are very likely associated with volcanic eruptions (Shalygin et al., 2015).

Venus was also studied accidentally, for example with the Solar and Heliospheric Observatory (SOHO), a mission dedicated to observe the solar weather. In June 1996 the CTOF detector of the CELIAS mass spectrometer picked up unusually high fluxes of C^+ and O^+ ions near Earth's L1 point, with speeds comparable to the one of the solar wind. The ions were coming from downstream Venus, which was at a distance of 45 million kilometers from SOHO at that time. The heavy ions originate from the ionosphere region of Venus rather than the corona according to their energy distribution. (Grünwaldt et al., 1997).

More Venus flybys were performed by the Messenger spacecraft in 2006 and 2007 on its way to Mercury. Messenger took images of the cloud covered planet (Johnson and de Oliveira, 2019). The clouds consist mainly of sulfuric acid droplets and are separated into three layers in-between 40 to 80 km above the surface. The existence of the cloud cover was well known before the first Venus missions as Venus appeared featureless in the visible wavelength range when observed through a telescope. This led to quite some speculations about what could be hidden beneath the clouds (Kasprzak, 1990). But as the lander missions showed that Venus neither has an ocean nor any other water source, it is also in many other aspects a deadly planet. The surface temperature lies above 730 K, the pressure exceeds the one on Earth by a factor of 90 and the atmosphere consists, apart from the acidic clouds, almost entirely of carbon dioxide (Williams, 2016).

However hostile for terrestrial life the planet may seem, the question whether Venus hosts life is as old as the Venus missions itself or even older. In 1967 Morowitz and Sagan (1967) published an article on the possibility of life being present in the sulfuric acid droplets in Venus' clouds. At first the idea may seem improbable that life could exist in such an unpleasant environment. However, as they pointed out, all ingredients needed for photosynthesis are present: water, carbon dioxide and sunlight. The temperatures in the cloud layer are in the range of 210 to 280 K, water vapor is assumed to exist and the pressure decreased to around 1 bar at this altitude. The lifeforms proposed by Morowitz and Sagan (1967) were hydrogen filled bladders floating in the atmosphere. They could collect water when it rains or when getting in contact with water droplets. Their underside could be sticky such that it could capture minerals that are blown up from the surface. These organisms would have a minimum diameter of at least 4 cm but could easily be bigger.

At that time the lower clouds of Venus were the most promising extraterrestrial environment to host life as their conditions came closer to those on Earth than any other known environment in our solar system. Today, we know of places that provide even better conditions of life, i.e. Europa, Titan and Enceladus, moons of Jupiter and Saturn (Cottin et al., 2017). But Venus moved back into the center of attention when in 2020 Greaves et al. (2020) reported a detection of phosphine (PH_3) gas in the clouds of Venus. The single-line millimeter-waveband spectral observations were conducted with ALMA and JCMT. An abundance of ~ 20 ppb was derived above the top of the clouds at

around 80 km above the surface. Any amount of phosphorus should be in oxidized form and up till now there is no known chemical, geological or other abiotic process which could explain the observed amount of PH_3.

On Earth, phosphine is mainly produced by anaerobic bacteria, which turns it into a bio marker and hence explains the excitement about the reported abundance. This again boosted questions about microbial life being present in the Venus cloud drops. In 2018 Limaye et al. (2018) stated that terrestrial-type microorganisms could survive in the lower cloud layers of Venus, as the conditions present (pressure of 1 atm, temperature of $\sim 60^{\circ}C$) are more moderate compared to the surface of Venus. The organisms could even contribute to the spectral signatures of Venus' clouds. Taking several terrestrial microorganisms like the A. *ferrooxidans* or green sulfur bacteria into account Limaye et al. (2018) proposed an iron- and sulfur-focused metabolic redox reactions that could take place in Venus' clouds. Microorganisms which depend on a water source might be confined to the interior of the cloud droplets as they otherwise risk drying out, as explained by Seager et al. (2020). Venus' atmosphere is very dry, and any microbes containing water would sooner or later reach an equilibrium with their surroundings. They could overcome this problem by being able to survive as spores, but this does not change the fact that the atmosphere of Venus is over an order of magnitude drier than the driest environments on Earth (Seager et al., 2020). Together with the very low pH this might not seem as the ideal place to look for life, but one has to keep in mind that also Earth hosts hostile environments where certain microbes were found to thrive. Especially in acid mine drainage acidophiles can be found to cope with $pH = 0$ conditions by keeping their intercellular pH level at a constant higher level. They achieve this by continuously pumping protons out of their cells and protecting their proteins from denaturation by including more amino acids with neutral side-groups (Rampelotto, 2010).

The current study deals with the atmospheric composition and the plasma environment of Venus and is divided into three parts. In a first part, possible measurements with the neutral gas mass spectrometer STROFIO on-board BepiColombo during its second Venus flyby in August 2021 are presented. The results are based on a model for the upper atmosphere of Venus previously published in Gruchola et al. (2019). A description of the model is given in the following Section 2. In addition to BepiColombo, also Solar Orbiter will have a Venus flyby in August 2021. The second part of this study will cover possible measurements of the Solar Wind Analyser (SWA) during the flyby. In a last part, the recently reported phosphine detection by Greaves et al. (2020) will be addressed by presenting an extension of our atmospheric model to include phosphine and its implication for future Venus missions, striving to detect phosphine *in situ* with mass spectrometers.

2. Model description

An exospheric model was used to calculate density profiles of 23 thermal species of the atmosphere and 4 hot neutral species, resulting from photo-dissociation of atmospheric parent molecules (Gruchola et al., 2019). The model is based on a Monte-Carlo simulation package previously developed for Mercury and the Moon (Wurz and Lammer, 2003; Wurz et al., 2007). The program is, strictly speaking, only applicable to the exosphere, a region where collisions can be neglected and the scale height is mass dependent and smaller than the mean free path.

The exobase is located at around 210 km on the days side and sinks to around 154 km on the night side. The Sun heats up the atmosphere on the day side, resulting in larger scale heights (Kasprzak et al., 1997). However, in situ observations were mostly conducted in the lower atmospheric regions below the homopause and well below the exobase. It was therefore necessary to analytically extrapolate the results to the exosphere and analyze the effect neglecting the collisions might have.

In the homosphere, species tend to have constant mixing ratios and the same, mass-independent scale heights. With recent carbon dioxide measurements in Venus' mesosphere conducted by SOIR on-board Venus Express the homopause was located in-between 124 to 134 km (Mahieux et al., 2012). Measurements with the VEX spectrometer SPICAV yielded similar results and showed that the homopause altitude varies between 119 to 138 km on the night side (Piccialli et al., 2015). The homopause is therefore not a sharp boundary and furthermore it is itself species dependent (von Zahn et al., 1983), located higher up for lighter species. On Venus, the mixing ratios are not constant throughout the whole homosphere because of the presence of cloud layers. The chemical composition in the clouds is affected by condensation and evaporation processes and thus is much different than in the remaining part of the homosphere, consisting mainly of sulphuric acid and water. The clouds furthermore form a chemically very active region in the atmosphere (Titov et al., 2018).

In regard of the problems mentioned above the simulations were started at 100 or 120 km above the surface, taking into account the mass of the species and its abundance and chemical processes in the clouds. This is explained in more detail in (Gruchola et al., 2019). As already discussed, a Monte-Carlo simulation was used, which takes a single particle, assigns to it a random direction and initial velocity according to a Poisson distribution around the most likely velocity of the Maxwell distribution. Then, by using discrete steps the program numerically computes the trajectory of the particle, analogously to how it has been done for e.g., Callisto's exosphere (Vorburger et al., 2015) or Mercury and the Moon (Wurz and Lammer, 2003; Wurz et al., 2007). The more time a particle spends at a given step the higher its density at this height. This is repeated for a certain number of particles, and if not stated otherwise

10^6 particles were used. Using a larger number of initial particles reduces the overall statistical uncertainty.

The calculation includes photochemical dissociation and ionization processes. Photochemical dissociation describes the process when solar UV radiation breaks up molecules in the atmosphere (Bertaux et al., 2007). The fragments produced in this process obtain a fraction of the binding energy according to their mass increasing the kinetic energy of the fragments. A higher kinetic energy implies a higher velocity which can be seen as a higher temperature. Most species in the Venusian exosphere therefore have two particle distributions, a thermal (cold) one and a hot one. The thermal particle distribution has a velocity which corresponds to the temperature of the atmosphere around it. In our program, the hot particle populations were simulated similar to the thermal ones but with a higher initial temperature resulting in higher initial velocities. The hot particle populations are therefore a key link for understanding atmospheric escape processes and photochemical dissociation plays a major role if it takes place above the exobase. Below, collisions prevent the particles from escaping the atmosphere.

The program does not include collisions nor some other processes taking place above the homopause like atmospheric sputtering, charge exchange, or photolysis. The program for Venus was developed mainly to study the heavy noble gases (Gruchola et al., 2019), which cannot undergo photochemical dissociation and have lower cross sections for charge exchange, and do not reach regions where sputtering becomes important.

The abundances used for the thermal and hot species are also summarized in (Gruchola et al., 2019). In addition, a phosphine population was included with a mixing ratio of 20 ppb at 80 km, and a lifetime of 10 s. This is the only species where simulations were not started at 100 or 120 km but below at 80 km. As phosphine was detected in the homosphere one could argue that the mixing ratio should stay constant up the homopause, however, the abundance of PH_3 appears to be strongly linked to the cloud region between ~ 40 to ~ 80 km and it comes not without difficulties to estimate the abundance at 100 km or even higher.

3. Results

3.1. BepiColombo

The ESA BepiColombo mission (BC) was launched in October 2018, and is currently on its way to Mercury. It consists of two scientific spacecraft, ESA's Mercury Planetary Orbiter (MPO) and JAXA's Mercury Magnetospheric Orbiter (MMO). It will have its first encounter with Mercury in October 2021 and it already completed one flyby at both Earth and Venus. The cruise phase includes in total six Mercury flybys, two Venus flybys and one Earth flyby. After the cruise phase BC will be captured by Mercury's gravity into a polar orbit around the planet in late 2025 (McKenna-Lawlor et al., 2018; Steiger et al., 2020).

BepiColombo will investigate the magnetosphere, the interaction of the solar wind (SW) with the atmosphere, it will conduct radio-science and plasma particle experiments and study the atmospheric composition. The MPO module hosts 11 scientific instruments, one of which is SERENA (Search for Exospheric Refilling and Emitted Natural Abundance), a suite of four instruments designed for particle detection in the Hermean environment. One of the instruments of SERENA is STROFIO (Start from a Rotating Field Mass Spectrometer), a mass spectrometer partially developed at the University of Bern (Orsini et al., 2021).

STROFIO is a neutral gas mass spectrometer based on a rotating electric field which will investigate the thermal exospheric gas composition of Mercury. It measures the mass over charge ratio (m/q_0) by a time-of-flight (TOF) technique. It can perform a quantitative analysis and resolve the chemical and elemental composition on both day and night side. The in situ measurements will give a better understanding of the dynamics in the atmosphere. STROFIO has a mass resolution of $m/\Delta m > 60$ and can detect neutral particles in the lowest energy range between ~ 0 to a few eV. It can detect masses in the range from 1 to 64 amu and has a temporal resolution of 10 s. STROFIO is furthermore characterized by a high sensitivity, a countrate of 0.14 counts per second will be produced by a particle density of 1 cm^{-3}. This corresponds to a sensitivity in excess of 1 mA/Torr (Orsini et al., 2010; Orsini et al., 2021).

The next upcoming milestone for BepiColombo is the second Venus flyby in August 2021 with a closest approach of 550 km. Our model makes predictions on what STROFIO could measure if the flyby operations of BepiColombo allow switching STROFIO on during the second Venus flyby. The first Venus flyby of BepiColombo took place in October 2020, but with a closest approach of over 10'000 km only little signal from in situ measurements would have been expected. In Fig. 1 a simulated mass spectrum of the thermal particle populations at 550 km above the surface with an integration time of 100 s is shown. At this altitude, out of 23 thermal species only 3 species and some of their isotopes still have a high enough abundance for a detection, i.e., hydrogen (H), molecular hydrogen (H_2), deuterium (D), hydrogen deuteride (HD) and helium (He).

In addition to the thermal species STROFIO could also measure the hot particle populations. In Fig. 2 a simulated mass spectrum of the hot species at 550 km above surface with an integration time of 100 s is shown. According to our model STROFIO could measure all of the four simulated hot particle populations during its closest approach.

The spectra shown in Figs. 1 and 2 show possible measurements for STROFIO at closest approach. Naturally, STROFIO could also be operated before and after, to obtain a more complete picture. This would especially yield insight into the escape processes and the dynamics of the

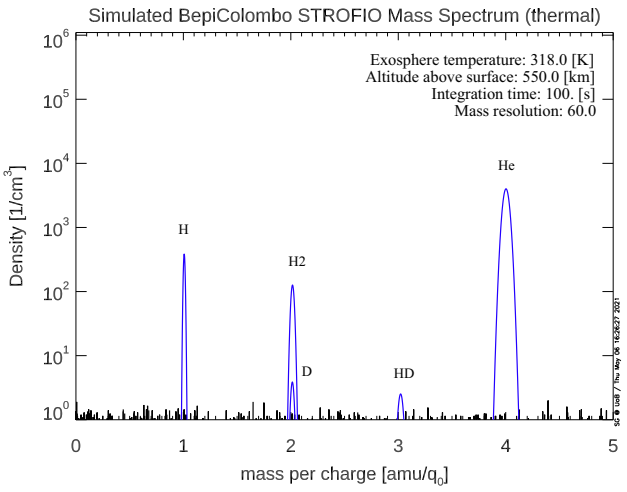

Fig. 1. Simulated STROFIO Venus mass spectrum of thermal species at an altitude of 550 km above the surface with an integration time of 100 s. Mass resolution $m/\Delta m = 60$.

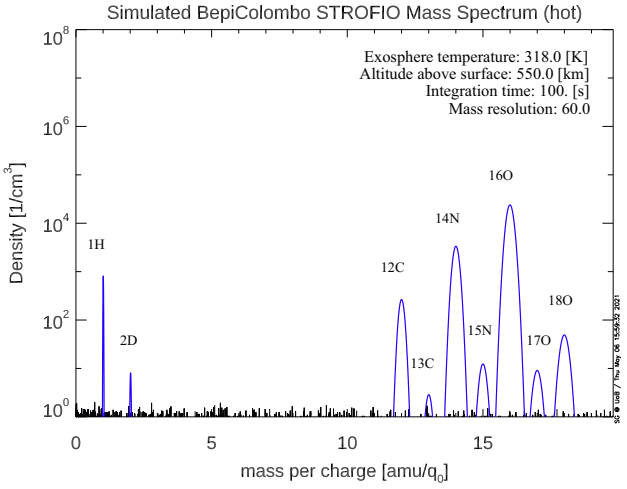

Fig. 2. Simulated STROFIO Venus mass spectrum of hot species at an altitude of 550 km above the surface with an integration time of 100 s. Mass resolution $m/\Delta m = 60$.

upper atmosphere of Venus. In Fig. 3 the number density profiles of the hot species H, C, N and O are given to estimate up to which altitudes signal can be expected. Even at 2500 km above the surface STROFIO should still be able to measure all four major hot species H, C, N and O (no isotopes), and even at 9000 km the hot hydrogen and oxygen components should still be visible. In case it is not possible to switch on STROFIO during closest approach it could maybe at least be switched on before and after to gather some data about the hot particle populations. The thermal hydrogen population (not shown in Fig. 3) should also be detectable at least up to 9000 km above the surface. The detection limits given in Fig. 3 were estimated based on the background levels of GCRs and galactic and interplanetary UV background given in Orsini et al. (2021). The signal-to-noise ratio during an intense SEP is expected to be much lower, however, these events are not expected to take place frequently (Orsini et al., 2021).

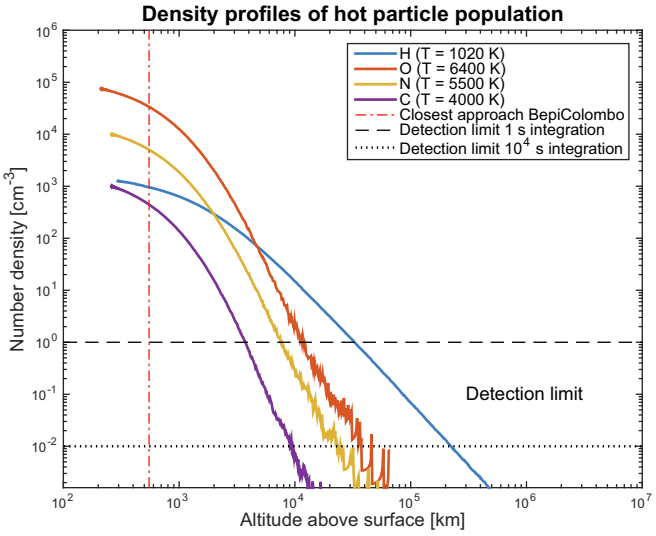

Fig. 3. Density profiles of the hot particle population. The planned closest approach of BepiColombo at 550 km above the surface during its seconond Venus flyby in August 2021 is indicated. The detection limits correspond to a 1 s and a 10^4 s integration, respectively. The species dependent temperatures are indicated in the legend. More information about the conduction of the corresponding simulations can be found in (Gruchola et al., 2019).

BepiColombo also carries the plasma instruments PICAM (Planetary Ion CAMera) and MPPE (Mercury Plasma/Particle Experiment), sensitive in the low and high energy ranges, respectively. During the first Venus flyby both instruments were switched on. PICAM, like STROFIO, is part of the SERANA suit and was developed to derive the exo-ionosphere extension and composition, and the close-to-planet magnetospheric dynamics of Mercury. It is sensitive to ions in the 1 eV to 3 keV energy range and together with data obtained by STROFIO the neutral to ion particle density will be derived to estimate the coupling between exo-ionosphere and exosphere, and its dependence on external conditions (Orsini et al., 2010).

MPPE is a comprehensive instrument package for plasma, high-energy particle and energetic neutral atom measurements and consists of seven sensors. During the first Venus flyby MPPE-MIA (Mercury Ion Analyzer) and MPPE-MEA1 (Mercury Electron Analyzer) verified that the trajectory led through the magentosheath as two plasma boundaries, the bow shock and the ion composition boundary, were crossed (https://global.jaxa.jp/press/2020/11/20201104-1_e.html#anchor03). The trajectory of the first Venus flyby was very similar to the planned trajectory of Solar Orbiter during its second Venus flyby which can be seen in Fig. 4 in Section 3.2. Both MMPE-MIA and MMPE-MEA1 are sensitive to ions and electrons, respectively, in the 5 eV/q to 30 keV/q energy range (Saito et al., 2010).

PICAM and MMPE will also be switched on during the second Venus flyby of BepiColombo. However, the trajectory will mostly lead through the magnetosheath without crossing plasma boundaries, as can be seen in Fig. 4 in Sec-

tion 3.2. Only on the day side it will pass through the ionosphere for a short amount of time. The closest approach of 550 km is around 100 km below the ionopause on the day side at solar minimum conditions (Martinecz et al., 2008).

3.2. Solar Orbiter

Solar Orbiter (SolO), an ESA mission with strong participation of NASA, was launched in the beginning of 2020. Its aim is to study the solar wind, the coronal magnetic field, the energetic particle radiation produced by solar eruptions and the solar dynamo (Müller et al., 2020). Solar Orbiter will perform in total one gravity assist (GAM) at Earth and 7 gravity assists at Venus to decrease its perihelion distance. The first Venus flyby already took place in December 2020, the next one is planned for 9 August 2021. It will enter a resonance orbit with Venus which together with the gravity assists will increase the inclination of its orbit around the Sun. This will allow Solar Orbiter to take the first ever close-up pictures of the polar regions of the Sun (Müller et al., 2020).

The payload of Solar Orbiter includes 10 scientific experiments, including 4 in situ instruments. Among them is the Solar Wind Analyser (SWA), designed to study the ionized particles of the solar wind (Müller et al., 2020). The solar wind consist mainly of protons (H^+, $\sim$ 96 %) and alpha particles (He^{++}, $\sim$ 4 %). Heavy ions (carbon and heavier) make up around 1 permille of the solar wind ion density (Wurz, 2005).

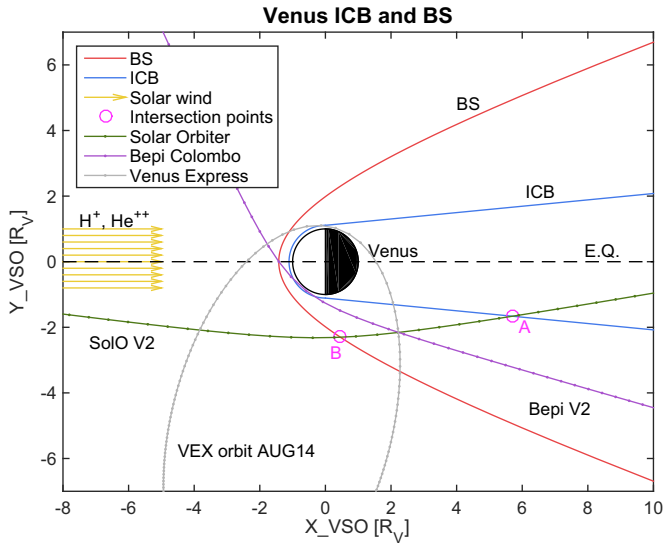

Fig. 4. Venus with fitted bow shock (BS) and ion composition boundary (ICB) derived from VEX observations, reproduced from Martinecz et al. (2008). In addition, the Solar Orbiter and BepiColombo trajectories during their second Venus gravity assists (V2) are indicated, obtained with SPICE kernels. Closest approach will take place on 9th of August 2021 for SolO and one day later on the 10th of August 2021 for BepiColombo. For reference, part of a VEX orbit, as it took place in the beginning of August 2014, is indicated as well. The tick marks show intervals of 5 min. The points A and B show the intersections of the SolO trajectory with the ICB and the B.S, respectively.

The solar wind also contains He^+ pickup ions. They originate from neutral helium ions flowing into the heliosphere as our solar system moves through the local interstellar medium. The Sun focuses these atoms gravitationally, which leads to the formation of a downwind cone. Helium atoms that get ionized in this cone become part of the solar wind. The flux peaks in the downwind direction. From the density of He^+ pickup ions in the solar wind one can derive an estimate of the neutral He density (Gloeckler et al., 2004). The SWA suite further consists of an Electron Analyser System (SWA-EAS), a Proton and Alpha particle Sensor (SWA-PAS), and a Heavy Ion Sensor (SWA-HIS). The SWA-HIS instrument will measure heavy ions from He up to Fe with energies in the range of 0.5 to 100 keV/e (Owen et al., 2020).

Even though SWA-HIS is designed to measure the solar wind ions, it can theoretically measure ions originating from any source if the ion energies lie in the required energy and mass range. And as SolO will use Venus for several gravity assists it will be exposed to the plasma environment of the planet. Our idea is to use this opportunity and switch on the SWA-HIS instrument during one of the flybys.

As Venus lacks an intrinsic magnetic field the solar wind interacts directly with the ionosphere. This leads to ionospheric outflow (Futaana et al., 2017). And as mentioned before, this outflow has even been measured at a distance of 45 million kilometers from Venus with the CTOF detector on-board the SOHO spacecraft. SOHO measured unusually high fluxes of C^+ and O^+ ions, with the abundance of C^+ being ≈ 10 % of the O^+ abundance. The C^+ and O^+ ions had roughly the same speed as the solar wind and are believed to originate in the ionospheric region of the planet rather than the corona. The fluxes of those heavy ions measured in addition to the solar wind were determined to be $(2.4 - 4.4) \cdot 10^3 cm^{-2} s^{-1}$ (Grünwaldt et al., 1997). The O^+ escape flux in the near Venus tail was also observed by the plasma instrument ASPERA-4 and the MAG magnetometer on-board VEX (Barabash et al., 2007).

Martinecz et al. (2008) used data obtained by the plasma analyzer Aspera-4 on-board Venus Express (VEX) to study the interaction between the solar wind and the ionosphere and located two important plasma boundaries, the Bow Shock (BS), and the Ion Composition boundary (ICB). The Bow Shock is a fast magnetosonic shock wave created by the supersonic solar wind. When VEX crossed the BS an increased intensity of energetic electrons with respect to the solar wind was measured. The BS marks the outer boundary of the magnetosheath, where the solar wind slows down and heats up. After crossing the BS and passing through the magnetosheath VEX crossed another plasma boundary, the ICB. It separates hot magnetized plasma of the magnetosheath from the thermal plasma of the ionosphere and was identified by the vanishing of the solar wind protons and the appearance of planetary ions. These planetary

ions are of low energy compared to the ions in the magnetosheath. Only inside the ICB significant fluxes of heavy ions can be observed. On the day side, the ICB corresponds approximately to the ionosphere. After crossing the ICB for the first time VEX crossed it again later, entering once more the magnetosheath, followed by a second crossing of the BS (Martinecz et al., 2008).

From the data obtained by VEX, Martinecz et al. (2008) inferred fits for the geometry of the BS and ICB. Those fits are reproduced in Fig. 4. For the bow shock region, a fit of the form

$$r = \frac{L}{1 + \epsilon \cos(\theta)} \tag{1}$$

was applied, with $L = 1.303\ \mathrm{R}_V$ and $\epsilon = 1.056$. The polar coordinates (r, θ) were measured with respect to a focus located at $(x_0, 0, 0) = (1.788, 0, 0)$ (Martinecz et al., 2008). To the ICB two fits were applied, one for the day side and one for the night side, as no single conic function could fit the data on both sides. As mentioned before the ICB on the day side corresponds approximately to the ionosphere. The fit on the day side is therefore a simple semi-circle with a radius of $r_c = 1.109\ \mathrm{R}_V$. With $\mathrm{R}_V \approx 6051$ km this locates the ICB boundary on the day side at approximately 660 km above the surface. On the night side the data were fitted by a linear regression with $y_1 = k_1 x + d_1$, with $k_1 = 0.097$ and $d_1 = 1.109$ for the upper ICB in Fig. 4 and $y_2 = k_2 x + d_2$, with $k_2 = -0.097$ and $d_1 = -1.109$ for the lower ICB (Martinecz et al., 2008).

Furthermore, Fig. 4 shows the direction of the solar wind, coming from the left and containing mainly protons and alpha particles. As the aim of this section is to give an estimate on what Solar Orbiter could measure during its second Venus gravity assist its trajectory (V2), obtained with SPICE kernels, is shown in Fig. 4. The reason why only V2 was included is that with exception of V1, which recently took place in the end of December 2020, gravity assist V3 to V7 do not cross the ICB and BS boundaries. V2, on the other hand will do exactly this which is a good opportunity to study the fluxes of planetary pickup ions in the magnetosheath (Sánchez Pérez and Varga, 2018). During V1 STROFIO was not switched on, however, several other instruments were, among them the magnetometer MAG. It was designed to study the solar and interplanetary magnetic fields, detect shock waves and learn more about energy fluctuations in the plasma. During V1 it was exposed to the illumination of both the Sun and Venus, but consistent sensor alignment was ensured by a careful choice of material which minimized effects of thermal expansion. As V1 took place recently in the end of December 2020 it is too early to say anything about the outcome of the flyby measurements (Horbury et al., 2020).

The trajectory V2 will cross both the BS and the ICB two times, however, in Fig. 4 only the latter intersections, A and B, are shown. Latter, because in Fig. 4 SolO is approaching Venus from the right. The spacecraft will therefore cross the BS and the ICB also in two other points, let's call them C and D. They are not shown in Fig. 4 for two reasons. First of all, the intersections will take place at large distances from Venus, approximately 50 Venus radii for point D (first crossing of ICB) and over 1000 Venus radii for point C (first crossing of BS). This would make Fig. 4 highly unreadable. Second, it doesn't seem safe to assume that the fits of the BS and the ICB are valid up to such large distances, and in addition the boundaries become more and more broadened the further away one gets from Venus. It is therefore questionable whether one can still talk about an intersection of the trajectory with the BS and the ICB so far away from Venus. The calculations below therefore focus on points A and B.

The model of Venus' upper atmosphere published in (Gruchola et al., 2019) deals with neutral particles, but ionization processes are included and therefore the model predicts production rates for ionized species. The planetary ions which reach the magnetosheath were ionized by the Sun on the day side and above the ICB. Therefore, we only considered species that reach altitudes of around 660 km above the surface. Furthermore, the planetary protons were not included as they cannot be distinguished from the solar wind protons and SWA-HIS only measures species from helium to iron. This left us with He^+, C^+, N^+ and O^+, contributed by Venus' atmosphere. Ions above the ICB on the day side are subject to the direct interaction with the solar wind. The convection electric field $\mathbf{E} = -\mathbf{v} \times \mathbf{B}$, with $\mathbf{v}$ the solar wind speed and $\mathbf{B}$ the draped interplanetary magnetic field, accelerates the ions to energies up to twice the energy of the solar wind, high enough to escape the planetary atmosphere (Luhmann et al., 2007; Futaana et al., 2017). These ions, henceforth called pickup ions, are dragged along with the solar wind and experience an acceleration in the direction of the convection electric field. The asymmetry of this field influences the direction of the pickup ion escape fluxes (Jarvinen et al., 2009). In this study, the asymmetrical nature of the convection electric field was not taken into account and the pickup ions are assumed to follow the same trajectory as the solar wind flux in the tail of Venus. Although this is a simplification, we note that the pickup ions from Venus' atmosphere have been observed near Earth orbit downstream of Venus (Grünwaldt et al., 1997).

We made predictions on what is to be expected for the ion fluxes when SolO crosses the BS boundary at point B and when it crosses the ICB at point A (see Fig. 4). The flux f_A through area A is given by

$$f_A = \frac{1}{A} \int_{ICB}^{BS} n(z) \cdot i \cdot A_{prod}(z)\, dz \tag{2}$$

$$\Longleftrightarrow f_A = \frac{i}{A} \int_{ICB}^{BS} n(z) \cdot A_{prod}(z)\, dz, \tag{3}$$

with $n(z)$ = number density at altitude z [m^{-3}], i = ionization rate [s^{-1}], A = area through which flux is to be calculated, $A_{\mathrm{prod}}(z)$ = area at altitude z where ions are produced. The production area can be written as

Table 1
ionization rates at solar minimum conditions used to calculate ion fluxes (Huebner et al., 1992).

Species	Ionization rate [s^{-1}]
He	$1.08 \cdot 10^{-7}$
C	$8.28 \cdot 10^{-6}$
N	$3.61 \cdot 10^{-7}$
O	$4.54 \cdot 10^{-7}$

$A_{\text{prod}}(z) = 2\pi \cdot (R_V + z)^2$ (half the surface of a sphere), with a Venus radius of $R_V = 6.051 \cdot 10^6$ m. The integration boundaries were set to $ICB = 660$ km and $BS = 1800$ km. The ionization rates used are summarized in Table 1 and were taken from https://phidrates.space.swri.edu (Huebner et al., 1992), corresponding to solar minimum conditions.

The ions produced on the day side above the ICB are carried downwind by the solar wind. When passing through the doughnut-shaped area at point B they will later also pass through the area at point A (assuming no losses occur). The areas are summarized in Table 2 and were calculated by subtracting the area enclosed by the ICB from the one enclosed by the BS.

As the area at location A is larger than at location B the flux decreases. This behavior is shown in Fig. 5. The crossing points C and D marked in Fig. 5 were obtained by assuming the fits of the BS and ICB to be valid up to great distances form Venus. They are merely marked to visualize the decrease in ion flux with larger distance.

A fit of the form

$$f(x) = \frac{1}{ax^3 + bx^2 + cx + d} \tag{4}$$

was applied to the ion fluxes at points A through D, with $a \approx 1.7375 \cdot 10^{-9}$, $b \approx 4.9081 \cdot 10^{-5}$, $c \approx 0.0014$ and $d \approx 0.0012$, shown by the green dashed line in Fig. 5. However, since SWA-HIS was designed to measure the high energetic solar wind particles it will not be able to measure the low energetic planetary ions in-between the ICB's. But the high energetic planetary pickup ions in the magnetosheath, accelerated by the solar wind, are visible to SWA-HIS. The measurable planetary pickup ion flux is shown in Fig. 5 by the solid green line with respect to the dashed green line indicating the fit.

The expression for the number density $n(z)$ of thermal species can be found by applying a fit of the form $\exp(az + b)$ to the density profile. For He the fit applied

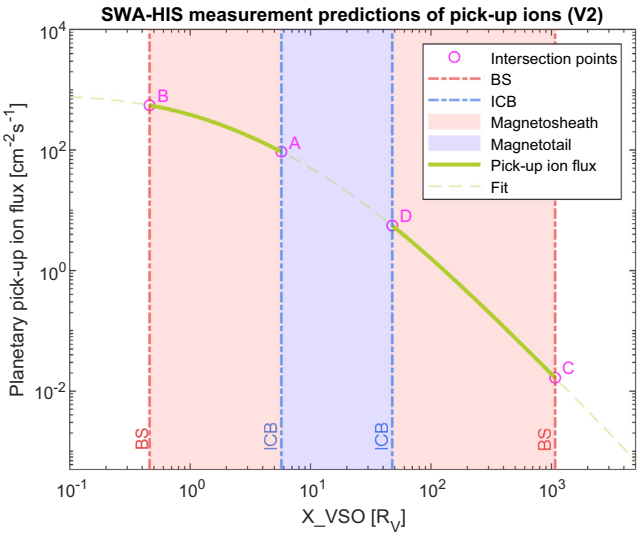

Fig. 5. SWA-HIS measurements predictions for the total ion flux of planetary pickup ions during SolO's second Venus gravity assist. While the spacecraft is inside the magnetosheath, in-between bow shock (BS) and ion composition boundary (ICB), it could measure energetic planetary ions. While in the magnetotail in-between the ICB's only low energetic planetary ions are abundant to which SWA-HIS is blind. Points A through D mark the intersections of the SolO trajectory with either BS or ICB.

is $n(z) = \exp(-2.15 \cdot 10^{-5}\ \text{m}^{-1} z + 33.94)$ with the parameters $a = 2.15 \cdot 10^{-5}\ \text{m}^{-1}$ and $b = 33.94$ taken from Gruchola et al. (2019). Inserting this expression into Eq. (3) the integral can be solved analytically. The results for the Helium fluxes derived in such a manner are summarized in Table 3.

To the density profiles of species of the hot population no fit was applied, as the calculations reached high enough altitudes and a simple interpolation sufficed. This on the other hand required the numerical integration form of Eq. (3), given in Eq. (5). It was used to calculate the fluxes of the pickup ions of the hot particle population. The step size Δz was set to 1 m.

$$f_A = \frac{1}{A} \sum_{z=ICB}^{BS} n(z) \cdot i \cdot A_{prod}(z)\, \Delta z \tag{5}$$

The fluxes predicted by our model are summarized in Table 3 at locations A and B for four species.

With a typical solar wind flux scaled to the Venus orbit at 0.7 AU of $\sim 8 \cdot 10^8$ cm^{-2}s^{-1} (Wurz, 2005) the ion fluxes of energetic planetary ions produced by the solar wind cor-

Table 2
Coordinates of crossing points A and B marked in Fig. 4. Points correspond to Solar Orbiter crossing the ICB and BS, respectively.

Point	X_VSO [R_V]	Y_VSO [R_V]	Area [R_V^2]	Area [cm^2]
A	5.72 ± 0.01	−1.66 ± 0.01	69.78 ± 0.33	$(2.555 \pm 0.012) \cdot 10^{19}$
B	0.46 ± 0.01	−2.31 ± 0.01	11.80 ± 0.16	$(4.319 \pm 0.058) \cdot 10^{18}$

Table 3
Ion fluxes expected for SWA-HIS during second Venus gravity assist. Fluxes are given in units of $cm^{-2}s^{-1}$.

Point	He^+	C^+	N^+	O^+	Total
A	21.13 ± 0.10	11.319 ± 0.054	6.521 ± 0.031	54.58 ± 0.26	93.55 ± 0.28
B	125.06 ± 1.69	66.96 ± 0.90	38.58 ± 0.52	322.89 ± 4.36	553.49 ± 4.79

respond to roughly 0.7 ppm of the solar wind flux at point B. With the effective area of the pixels of SWA-HIS one can further estimate the total count rates which are to be expected while SolO passes through the magnetosheath in-between points A and B. The effective area A_{eff} of one pixel of SWA-HIS can be obtained with the geometrical factor, $G = 1 \cdot 10^{-5}$ cm^2 sr eV/eV, the pixel resolution, 0.011 sr, and the energy resolution, $\Delta E/E = 0.09$ eV/eV (Owen et al., 2020), and equals roughly $A_{\text{eff}} \approx 0.01$ cm^2. Multiplied with the actual fluxes this yields the expected counts per second. According to SPICE kernel data SolO will spend around 45 min (2700 s) in the magnetosheath between points A and B, during which SWA-HIS will be able to measure the planetary pickup ion fluxes. The ion count rates at points A and B are approximately 1 count per second and 5 counts per second, respectively. Summed up over the 2700 s and integrated over the whole angular distribution this yields total counts of planetary pickup ions of the order of $\mathcal{O}(10^3)$ to $\mathcal{O}(10^4)$.

The expected ion counts for SWA-HIS during 5 min after crossing the ICB at point A were simulated by assuming solar wind plasma conditions in the magnetosheath and are shown in Fig. 6. As SWA-HIS can detect ions from He up to Fe no hydrogen signal is visible. The predicted signal of the heavy ions C^+, N^+ and O^+ can be seen in the right end of the Figure. The planetary pickup He^+ is not expected to be distinguishable from the signal of the solar wind. For C^+, N^+ and O^+ on the other hand there is no solar wind background. Even if the ion count rates are low SWA-HIS should still be able to record signal as it can detect single ions. The predicted ion counts in Fig. 6 were calculated by using the fluxes given at point A (summarized in Table 3), at point B there is approximately a factor 5 more signal to be expected. As mentioned above, SWA-HIS will spend roughly 45 min in the magnetosheath in-between points A and B.

As SWA-HIS can detect single ions and there is no significant background in singly ionized particles it seems perfectly possible for SWA-HIS to detect the planetary pickup ions of Venus. This would yield important insight about the outflow of planetary ions and the ionization processes in Venus' upper atmosphere. To obtain a coherent picture of Venus' plasma environment it is important to start the measurements before entering the magnetosheath in a region where only solar wind ions are present. Long and continuous series of measurements will help to detect the different ion populations and furthermore improve the model of the bow shock and the ion composition boundaries as they are subject to diurnal variations.

3.3. Phosphine

In September 2020, Greaves et al. (2020) reported the ground-based single-line PH_3 detection in Venus' cloud decks with ALMA and JCMT. An abundance of 20 ppb PH_3 around 80 km above the surface was deduced from the measurements. Since the first announcement of a possible phosphine detection, several studies questioning the reliability of the observations followed quickly. Snellen et al. (2020) for example see a problem in the 12th order polynomial fitting that was applied to the data. According to them, the data show no statistical evidence for phosphine in the atmosphere of Venus. Encrenaz et al. (2020) looked for signatures of phosphine in the infrared range and deduced a 3-σ upper limit of 5 pbb for the PH_3 mixing ratio, presumably constant throughout the atmosphere. This value is four times smaller than the one measured by Greaves et al. (2020) in the millimeter-waveband, but still more than could be explained by known geological or chemical processes. Villanueva et al. (2020) reanalyzed the data and found several fundamental issues in the analysis and interpretation of the spectroscopic data by Greaves et al. (2020). They did not find any evidence for phosphine, which is in agreement with a PH_3 abundance $<$ 5 ppb (3-σ).

The authors of Greaves et al. (2020) informed the editors of Nature Astronomy about an error in the original processing of the ALMA Observatory data. The re-

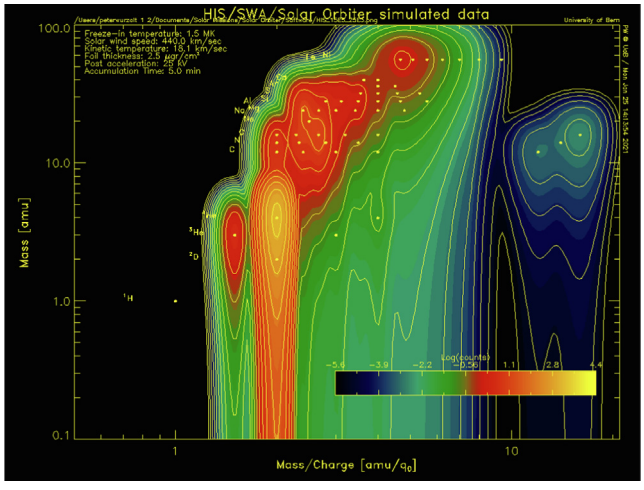

Fig. 6. Predicted ion counts of SWA-HIS during 5 min after crossing the ICB at point A. The dots represent the nominal position of the solar wind and Venus pickup ions.

calibration impacted the results and the data were reanalyzed. In the latest analysis, Greaves et al. (2021) report net abundances of phosphine of up to ~20 ppb above 55 km from the JCMT data, while from the ALMA data an abundance of ~7 ppb was deduced (signal loss possible) (Greaves et al., 2021).

Nevertheless, the discussion raised the question whether the species could be detected in the atmosphere of Venus by mass spectrometry. The model published in Gruchola et al. (2019) was hence extended to include phosphine and a number density profile was calculated, shown in Fig. 7. An abundances of 5 ppb at 80 km with a lifetime of 10 s above surface was used as input data for our model. The density profile for the initially reported abundance of 20 ppb is shown for reference. The detection limits indicated in Fig. 7 correspond to integration times of 1 s and 10^4 s, respectively, assuming the performance of a current generation neutral gas mass spectrometer (NGMS) (Wurz et al., 2012).

According to Fig. 7 a detection of phosphine below 170 km should be possible, however, the main obstacle to identifying PH_3 with mass spectrometry is the limited resolution. In Fig. 8 a modelled mass spectrum with mass range 33.5 to 36.5 amu/q_0 is shown, at an altitude of 130 km above surface with an integration time of 100 s and a mass resolution of $m/\Delta m = 1000$. The signals of PH_3 and its isotope PH_2D (negligible amounts of PHD_2 and PD_3 abundance at this altitude), the light blue peaks, are masked by other, more abundant species as the $^{16}O^{18}O$ isotope of O_2 and the Cl fragment of HCl. The spectrum was calculated at 130 km since the proposed ESA mission EnVision will reach this altitude through aerobraking. According to our model it would therefore not be possible for EnVision to measure PH_3. The predictions do not improve much at

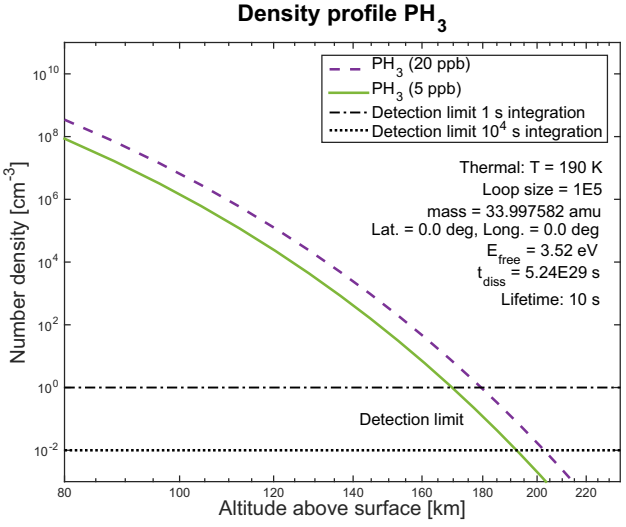

Fig. 7. Number density profile of phosphine at the equator at noon, starting from 80 km above the surface. Initial values: 20 ppb (Greaves et al., 2020) and 5 ppb (Encrenaz et al., 2020). Atmospheric temperature at 80 km above the surface taken from Ando et al. (2020).

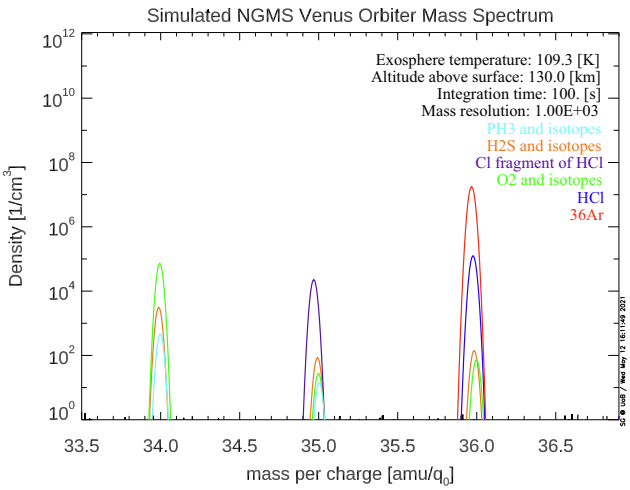

Fig. 8. Predicted mass spectrum at an altitude of 130 km above surface including the phosphine signal. The spectrum corresponds to an integration time of 100 s and a mass resolution of 1000

lower or higher altitudes, since the problematic species have a similar mass to phosphine (or its isotopes) and therefore their density profiles show a similar behavior.

The problem could be tackled by using a higher mass resolution to resolve the peaks shown in Fig. 8 separately. To resolve PH_3 and $^{16}O^{18}O$ a mass resolution of almost 10'000 is required (m_{PH_3} = 33.99758 u, $m_{^{16}O^{18}O}$ = 33.99407 u, $m/\Delta m = m_{PH_3}/(m_{PH_3} - m_{^{16}O^{18}O}) = 9697.61$). To resolve the peaks of PH_2D and the chlorine fragment of HCl a mass resolution of $m/\Delta m \approx 1000$ would be sufficient if both species would have approximately the same abundance. Fig. 8 was calculated with $m/\Delta m = 1000$ which is clearly not enough to resolve the two peaks.

However, one has to mention that the abundance of O_2 is unfortunately poorly established. Up till now no in situ measurements have been conducted above the cloud top. In the lower atmosphere estimations for the O_2 abundance range from 0 to 20 ppm (de Pater and Lissauer, 2010), 18 ± 4 ppm (Mukhin et al., 1983) and ⩽ 3 ppm (Krasnopolsky, 2006). The only measurements at higher altitudes were ground-based and conducted with a high-resolution long-slit spectrograph CSHELL at the NASA Infrared Telescope Facility (IRTF) on Mauna Kea, Hawaii, and an abundance of 5–8.6 ppm at 80 km was reported (Krasnopolsky, 2010). In addition to the problematic O_2 abundance, the isotope ratios have also not yet been measured accurately. Ground-based IR observations inferred $\delta^{18}O$ = 42 ± 85 ‰ (Iwagami et al., 2015), which corresponds to 95.8 ± 8.5 % of the standard abundance on Earth. For the simulated mass spectrum shown in Fig. 8 an initial O_2 abundance of 8.6 ppm at 120 km was used together with the same isotopic ratios for all species as on Earth, with the exception of H/D, for which a ratio of 100 was used (Bertaux and Clarke, 1989).

According to our model it is therefore equally unlikely that phosphine has been measured previously with the

Neutral Gas Mass Spectrometer (NGMS) on-board Pioneer Venus and not been reported due to misinterpretation of the results. Pioneer Venus probed the atmosphere while descending from an altitude of 62 km down to the surface (Hoffman et al., 1980). NGMS had a mass resolution of $m/\Delta m \approx 440$, not enough to resolve PH_3 and $^{16}O^{18}O$ or Cl and PH_2D. Unfortunately, the NGMS was a scanning mass spectrometer which only recorded signal at specific masses. It would be easier to tell which peaks correspond to which species if the full mass range would have been probed. One example is the signal measured at masses $m_1 = 33.992$ and $m_2 = 34.005$ amu/q_0. If those two masses should be resolved a mass resolution of around $m/\Delta m = m_2/(m_2 - m_1) \approx 2616$ would be required, much higher than the reported 440 (Hoffman et al., 1980). It is therefore much more likely that both signals belong to the same peak which might contain several unresolved species.

The discussion about phosphine in Venus' cloud decks is still ongoing but only future measurements will have the potential to show whether phosphine is truly present in Venus' clouds and, if it is, determine its origin.

4. Conclusions

The modelled thermal and hot particle populations predict possible measurements for the STROFIO instrument on-board BepiColombo during its second Venus flyby in August 2021. The spacecraft will pass Venus at an altitude of 550 km above surface at closest approach, where densities of thermal mono-atomic hydrogen, molecular hydrogen and helium as well as their isotopes should be measurable. In addition, the four hot particle populations of hydrogen, carbon, nitrogen and oxygen should be visible to STROFIO during the flyby. Measuring the abundances of the neutral particle populations in the upper atmosphere of Venus could yield more insight into the escape processes.

Solar Orbiter will pass by Venus in August 2021 for its third gravity assist, the second at Venus. It carries the SWA-HIS instrument, designed to study the solar wind ions in a large energy range. While passing by Venus Solar Orbiter will fly through the magnetosheath, a region between the bow shock and the ion composition boundary, where the solar wind picks up planetary ions and accelerates them to its wind speed. This turns them into energetic planetary ions that can be detected by SWA-HIS. Data that could be collected during this gravity assist would contribute to the knowledge of the ionization processes in the upper atmosphere and the outflow of planetary ions.

The Venus flybys of BepiColombo and Solar Orbiter will both take place in August 2021; first Solar Orbiter on August 9 and then BepiColombo on August 10. This is particularly interesting as the space environment encountered by the two spacecraft will most likely be very similar since the solar activity stays approximately constant over two days. Both spacecraft carry plasma instruments which can measure plasma boundaries like the bow shock and the ion composition boundary. This allows data on said boundaries to be obtained from two spacecraft at almost the same time.

Finally, the phosphine model shows that it is unlikely that PH_3 or any of its isotopes can be detected above the clouds with mass spectrometry. It seems also unlikely that phosphine has previously been measured with Pioneer Venus, as NGMS has a very limited mass resolution and it seems likely that $O^{16}O^{18}$ and the Cl fragment of HCl have a higher abundance that PH_3. The O_2 abundance is poorly established, but so is the abundance of PH_3. Until now it is not resolved whether the observations made by Greaves et al. (2020) do show a phosphine signal or not. Only a much higher mass resolution, $> 10'000$, will allow for its identification.

Declaration of Competing Interest

The authors declare that they have no known competing financial interests or personal relationships that could have appeared to influence the work reported in this paper.

Acknowledgments

This work is funded by the Swiss National Science Foundation (SNF).

References

Ando, H., Imamura, T., Tellmann, S., Pätzold, M., Häusler, B., Sugimoto, N., Takagi, M., Sagawa, H., Limaye, S., Matsuda, Y., Choudhary, R. K., Antonita, M., 2020. Thermal structure of the Venusian atmosphere from the sub-cloud region to the mesosphere as observed by radio occultation. Scientific Reports. https://doi.org/10.1038/s41598-020-59278-8.

Bailey, J. (2013). Mariner 2 and its Legacy: 50 Years on, 78. http://arxiv.org/abs/1302.3675. arXiv:1302.3675.

Barabash, S., Fedorov, A., Sauvaud, J.J., Lundin, R., Russell, C.T., Futaana, Y., Zhang, T.L., Andersson, H., Brinkfeldt, K., Grigoriev, A., Holmström, M., Yamauchi, M., Asamura, K., Baumjohann, W., Lammer, H., Coates, A.J., Kataria, D.O., Linder, D.R., Curtis, C.C., Hsieh, K.C., Sandel, B.R., Grande, M., Gunell, H., Koskinen, H.E., Kallio, E., Riihelä, P., Säles, T., Schmidt, W., Kozyra, J., Krupp, N., Fränz, M., Woch, J., Luhmann, J., McKenna-Lawlor, S., Mazelle, C., Thocaven, J.J., Orsini, S., Cerulli-Irelli, R., Mura, M., Milillo, M., Maggi, M., Roelof, E., Brandt, P., Szego, K., Winningham, J.D., Frahm, R.A., Scherrer, J., Sharber, J.R., Wurz, P., Bochsler, P., 2007. The loss of ions from Venus through the plasma wake. Nature. https://doi.org/10.1038/nature06434.

Basilevsky, A.T., Ivanov, M.A., Head, J.W., Aittola, M., Raitala, J., 2007. Landing on Venus: Past and future. Planet. Space Sci. https://doi.org/10.1016/j.pss.2007.09.005.

Bertaux, J.L., Clarke, J.T., 1989. Deuterium content of the Venus atmosphere. Nature. https://doi.org/10.1038/338567a0.

Bertaux, J.L., Vandaele, A.C., Korablev, O., Villard, E., Fedorova, A., Fussen, D., Quémerais, E., Belyaev, D., Mahieux, A., Montmessin, F., Muller, C., Neefs, E., Nevejans, D., Wilquet, V., Dubois, J.P., Hauchecorne, A., Stepanov, A., Vinogradov, I., Rodin, A., Nevejans, D., Montmessin, F., Fedorova, A., Cabane, M., Chassefière, E., Chaufray, J.Y., Dimarellis, E., Dubois, J.P., Hauchecorne, A., Leblanc, F., Lefèvre, F., Rannou, P., Quémerais, E., Villard, E., Fussen, D., Muller, C., Neefs, E., Van Ransbeeck, E., Wilquet, V.,

Stepanov, A., Vinogradov, I., Zasova, L., Forget, F., Lebonnois, S., Titov, D., Rafkin, S., Durry, G., Gérard, J.C., Sandel, B., 2007. A warm layer in Venus' cryosphere and high-altitude measurements of HF, HCl, H2O and HDO. Nature. https://doi.org/10.1038/nature05974.

Cottin, H., Kotler, J.M., Bartik, K., Cleaves, H.J., Cockell, C.S., de Vera, J.P.P., Ehrenfreund, P., Leuko, S., Ten Kate, I.L., Martins, Z., Pascal, R., Quinn, R., Rettberg, P., & Westall, F. (2017). Astrobiology and the Possibility of Life on Earth and Elsewhere.... doi:10.1007/s11214-015-0196-1.

Encrenaz, T., Greathouse, T.K., Marcq, E., Widemann, T., Bézard, B., Fouchet, T., Giles, R., Sagawa, H., Greaves, J., & Sousa-Silva, C. (2020). A stringent upper limit of the PH3abundance at the cloud top of Venus. Astronomy and Astrophysics, doi:10.1051/0004-6361/202039559. arXiv:2010.07817.

Futaana, Y., Stenberg Wieser, G., Barabash, S., Luhmann, J.G., 2017. Solar Wind Interaction and Impact on the Venus Atmosphere. https://doi.org/10.1007/s11214-017-0362-8.

Gloeckler, G., Möbius, E., Geiss, J., Bzowski, M., Chalov, S., Fahr, H., McMullin, D.R., Noda, H., Oka, M., Ruciński, D., Skoug, R., Terasawa, T., Von Steiger, R., Yamazaki, A., Zurbuchen, T., 2004. Observations of the helium focusing cone with pickup ions. Astron. Astrophys. https://doi.org/10.1051/0004-6361:20035768.

Greaves, J.S., Richards, A.M.S., Bains, W., Rimmer, P.B., Clements, D. L., Seager, S., Petkowski, J.J., Sousa-Silva, C., Ranjan, S., & Fraser, H.J. (2021). Recovery of spectra of phosphine in venus' clouds. arXiv:2104.09285.

Greaves, J.S., Richards, A.M.S., Bains, W., Rimmer, P.B., Sagawa, H., Clements, D.L., Seager, S., Petkowski, J.J., Sousa-Silva, C., Ranjan, S., Drabek-Maunder, E., Fraser, H.J., Cartwright, A., Mueller-Wodarg, I., Zhan, Z., Friberg, P., Coulson, I., Lee, E., & Hoge, J. (2020). Phosphine Gas in the Cloud Decks of Venus, http://arxiv.org/abs/2009.06593. doi:10.1038/s41550-020-1174-4. arXiv:2009.06593.

Gruchola, S., Galli, A., Vorburger, A., Wurz, P., 2019. The upper atmosphere of Venus: Model predictions for mass spectrometry measurements. Planet. Space Sci. 170. https://doi.org/10.1016/j.pss.2019.03.006.

Grünwaldt, H., Neugebauer, M., Hilchenbach, M., Bochsler, P., Hovestadt, D., Bürgi, A., Ipavich, F.M., Reiche, K.U., Axford, W.I., Balsiger, H., Galvin, A.B., Geiss, J., Gliem, F., Gloeckler, G., Hsieh, K.C., Kallenbach, R., Klecker, B., Livi, S., Lee, M.A., Managadze, G. G., Marsch, E., Möbius, E., Scholer, M., Verigin, M.I., Wilken, B., Wurz, P., 1997. Venus tail ray observation near Earth. Geophys. Res. Lett. https://doi.org/10.1029/97GL01159.

Gurnett, D.A., Kurth, W.S., Roux, A., Gendrin, R., Kennel, C.F., Bolton, S.J., 1991. Lightning and plasma wave observations from the Galileo flyby of Venus. Science. https://doi.org/10.1126/science.253.5027.1522.

Hoffman, J.H., Hodges, R.R., Wright, W.W., Blevins, V.A., Duerksen, K. D., Brooks, L.D., 1980. Pioneer Venus Sounder Probe Neutral Gas Mass Spectrometer. IEEE Trans. Geosci. Remote Sens. GE-18, 80–84. https://doi.org/10.1109/TGRS.1980.350286.

Horbury, T.S., O'Brien, H., Carrasco Blazquez, I., Bendyk, M., Brown, P., Hudson, R., Evans, V., Oddy, T.M., Carr, C.M., Beek, T.J., Cupido, E., Bhattacharya, S., Dominguez, J.A., Matthews, L., Myklebust, V.R., Whiteside, B., Bale, S.D., Baumjohann, W., Burgess, D., Carbone, V., Cargill, P., Eastwood, J., Erdös, G., Fletcher, L., Forsyth, R., Giacalone, J., Glassmeier, K.H., Goldstein, M.L., Hoeksema, T., Lockwood, M., Magnes, W., Maksimovic, M., Marsch, E., Matthaeus, W.H., Murphy, N., Nakariakov, V.M., Owen, C.J., Owens, M., Rodriguez-Pacheco, J., Richter, I., Riley, P., Russell, C.T., Schwartz, S., Vainio, R., Velli, M., Vennerstrom, S., Walsh, R., Wimmer-Schweingruber, R.F., Zank, G., Müller, D., Zouganelis, I., Walsh, A.P., 2020. The Solar Orbiter magnetometer. Astron. Astrophys. https://doi.org/10.1051/0004-6361/201937257.

Huebner, W.F., Keady, J.J., Lyon, S.P., 1992. Solar photo rates for planetary atmospheres and atmospheric pollutants. Astrophys. Space Sci. https://doi.org/10.1007/BF00644558.

Iwagami, N., Hashimoto, G.L., Ohtsuki, S., Takagi, S., Robert, S., 2015. Ground-based IR observation of oxygen isotope ratios in Venus's atmosphere. Planet. Space Sci. https://doi.org/10.1016/j.pss.2014.10.004.

Jarvinen, R., Kallio, E., Janhunen, P., Barabash, S., Zhang, T.L., Pohjola, V., Sillanpää, I., 2009. Oxygen ion escape from Venus in a global hybrid simulation: Role of the ionospheric O+ ions. Ann. Geophys. https://doi.org/10.5194/angeo-27-4333-2009.

Johnson, N.M., de Oliveira, M.R., 2019. Venus Atmospheric Composition In Situ Data: A Compilation. Earth and Space Science. https://doi.org/10.1029/2018EA000536.

Kasprzak, W. (1990). The Pioneer Venus Orbiter: 11 years of data. A Laboratory for Atmospheres Seminar Talk. NASA Technical Memorandum (100761).

Kasprzak, W., Keating, G., Hsu, N., Stewart, A., Colwell, W., Bougher, S., 1997. Solar activity behavior of the thermosphere. In: Venus II: Geology, Geophysics, Atmosphere, and Solar Wind Environment. University of Arizona Press, Tucson, pp. 225–257.

Krasnopolsky, V.A., 2006. Chemical composition of Venus atmosphere and clouds: Some unsolved problems. Planet. Space Sci. https://doi.org/10.1016/j.pss.2006.04.019.

Krasnopolsky, V.A., 2010. Venus night airglow: Ground-based detection of OH, observations of O_2 emissions, and photochemical model. Icarus. https://doi.org/10.1016/j.icarus.2009.10.019.

Limaye, S.S., Mogul, R., Smith, D.J., Ansari, A.H., Słowik, G.P., Vaishampayan, P., 2018. Venus' spectral signatures and the potential for life in the clouds. Astrobiology. https://doi.org/10.1089/ast.2017.1783.

Luhmann, J.G., Kasprzak, W.T., & Russell, C.T. (2007). Space weather at Venus and its potential consequences for atmosphere evolution. Journal of Geophysical Research E: Planets, doi:10.1029/2006JE002820.

Mahieux, A., Vandaele, A.C., Robert, S., Wilquet, V., Drummond, R., Montmessin, F., & Bertaux, J.L. (2012). Densities and temperatures in the Venus mesosphere and lower thermosphere retrieved from SOIR on board Venus Express: Carbon dioxide measurements at the Venus terminator. Journal of Geophysical Research E: Planets, doi:10.1029/2012JE004058.

Martinecz, C., Fränz, M., Woch, J., Krupp, N., Roussos, E., Dubinin, E., Motschmann, U., Barabash, S., Lundin, R., Holmström, M., Andersson, H., Yamauchi, M., Grigoriev, A., Futaana, Y., Brinkfeldt, K., Gunell, H., Frahm, R.A., Winningham, J.D., Sharber, J.R., Scherrer, J., Coates, A.J., Linder, D.R., Kataria, D.O., Kallio, E., Sales, T., Schmidt, W., Riihela, P., Koskinen, H.E., Kozyra, J.U., Luhmann, J., Russell, C.T., Roelof, E.C., Brandt, P., Curtis, C.C., Hsieh, K.C., Sandel, B.R., Grande, M., Sauvaud, J.A., Fedorov, A., Thocaven, J.J., Mazelle, C., McKenna-Lawler, S., Orsini, S., Cerulli-Irelli, R., Maggi, M., Mura, A., Milillo, A., Wurz, P., Galli, A., Bochsler, P., Asamura, K., Szego, K., Baumjohann, W., Zhang, T.L., Lammer, H., 2008. Location of the bow shock and ion composition boundaries at Venus-initial determinations from Venus Express ASPERA-4. Planet. Space Sci. https://doi.org/10.1016/j.pss.2007.07.007.

McKenna-Lawlor, S., Jackson, B., Odstrcil, D., 2018. Space weather at planet Venus during the forthcoming BepiColombo flybys. Planet. Space Sci. https://doi.org/10.1016/j.pss.2017.10.001.

Morowitz, H., & Sagan, C. (1967). Life in the clouds of venus? [3]. doi:10.1038/2151259a0.

Mukhin, L.M., Gel'man, B.G., Lamonov, N.I., Mel'nikov, V.V., Nenarokov, D.F., Okhotnikov, B.P., Rotin, V.A., Khokhlov, V.N., 1983. Gas-chromatograph analysis of the chemical compositionof the atmosphere of Venus by the landers of the Venera 13 and Venera 14 spacecraft. In: Cosmic Research (English translation of Kosmicheskie Issledovaniya).

Müller, D., St. Cyr, O.C., Zouganelis, I., Gilbert, H.R., Marsden, R., Nieves-Chinchilla, T., Antonucci, E., Auchère, F., Berghmans, D., Horbury, T.S., Howard, R.A., Krucker, S., Maksimovic, M., Owen, C. J., Rochus, P., Rodriguez-Pacheco, J., Romoli, M., Solanki, S.K., Bruno, R., Carlsson, M., Fludra, A., Harra, L., Hassler, D.M., Livi,

S., Louarn, P., Peter, H., Schühle, U., Teriaca, L., Del Toro Iniesta, J. C., Wimmer-Schweingruber, R.F., Marsch, E., Velli, M., De Groof, A., Walsh, A., & Williams, D. (2020). The Solar Orbiter mission: Science overview. doi:10.1051/0004-6361/202038467. arXiv:2009.00861.

Orsini, S., Livi, S., Torkar, K., Barabash, S., Milillo, A., Wurz, P., Di Lellis, A.M., Kallio, E., Kasper, J., McKenna, S., Vaisberg, O., Allegrini, F., Andersson, H., Aoustin, C., Asamura, K., Avanov, L., Babkin, V., Balaz, J., Balikhin, M., Balint, S., Baumjohann, W., Benz, W., Berthelier, J.J., Biernat, H., Brandt, P.C., Bruno, R., Burch, J., Capria, M.T., Castellano, M.G., Cerulli-Irelli, R., Collier, M.R., Cremonese, G., Crider, D., Curtis, C.C., D'Amicis, R., Daglis, I.A., Dandouras, I., de Angelis, E., de Los Santos, A., Delcourt, D., Delva, M., Desai, M., Di Cosimo, S., Duvet, L., Escoubet, P.C., Fama, M., Fedorov, A., Ferrari, L., Fraenz, M., Fremuth, G., Genzer, M., Gnoli, A., Goldstein, R., Grande, M., Grishin, V., Gurnee, R., Haggerty, D. K., Heerlein, K., Hernyes, I., Holmström, M., Hsieh, K.C., Ip, W.H., Lacques, A., Jeszensky, H., Johnson, R., Kecskemety, K., Killen, R., Koynash, G., Krupp, N., Kudela, K., Lajos, S., Lammer, H., Latini, G., Leblanc, F., Leblanc, F., Leibov, A., Leoni, R., Lichtenegger, H., Lipusz, C., Loose, A., Louarn, P., Lundin, R., Mälkki, A., Mangano, V., Massetti, S., Mattioli, F., McCann, D., McComas, D.J., Mitchell, D.G., Moore, T.E., Morbidini, A., Mura, A., Nilsson, H., Oja, M., Orfei, R., Panagopoulos, I., Piazza, D., Pitout, F., Pollock, C. et al. (2010). SERENA: A suite of four instruments (ELENA, STROFIO, PICAM and MIPA) on board BepiColombo-MPO for particle detection in the Hermean environment. Planetary and Space Science, doi:10.1016/j.pss.2008.09.012.

Orsini, S., Livi, S.A., Lichtenegger, H., Barabash, S., Milillo, A., De Angelis, E., Phillips, M., Laky, G., Wieser, M., Olivieri, A., Plainaki, C., Ho, G., Killen, R.M., Slavin, J.A., Wurz, P., Berthelier, J.-J., Dandouras, I., Kallio, E., McKenna-Lawlor, S., Szalai, S., Torkar, K., Vaisberg, O., Allegrini, F., Daglis, I.A., Dong, C., Escoubet, C.P., Fatemi, S., Fränz, M., Ivanovski, S., Krupp, N., Lammer, H., Leblanc, F., Mangano, V., Mura, A., Nilsson, H., Raines, J.M., Rispoli, R., Sarantos, M., Smith, H.T., Szego, K., Aronica, A., Camozzi, F., Di Lellis, A.M., Fremuth, G., Giner, F., Gurnee, R., Hayes, J., Jeszenszky, H., Tominetti, F., Trantham, B., Balaz, J., Baumjohann, W., Brienza, D., Bührke, U., Bush, M.D., Cantatore, M., Cibella, S., Colasanti, L., Cremonese, G., Cremonesi, L., D'Alessandro, M., Delcourt, D., Delva, M., Desai, M., Fama, M., Ferris, M., Fischer, H., Gaggero, A., Gamborino, D., Garnier, P., Gibson, W.C., Goldstein, R., Grande, M., Grishin, V., Haggerty, D., Holmström, M., Horvath, I., Hsieh, K.-C., Jacques, A., Johnson, R. E., Kazakov, A., Kecskemety, K., Krüger, H., Kürbisch, C., Lazzarotto, F., Leblanc, F., Leichtfried, M., Leoni, R., Loose, A., Maschietti, D., Massetti, S., Mattioli, F., Miller, G., Moissenko, D., Morbidini, A., Noschese, R., Nuccilli, F., Nunez, C., Paschalidis, N., et al., 2021. SERENA: Particle Instrument Suite for Determining the Sun-Mercury Interaction from BepiColombo. Space Sci. Rev. 217, 11. https://doi.org/10.1007/s11214-020-00787-3.

Owen, C.J., Bruno, R., Livi, S., Louarn, P., Al Janabi, K., Allegrini, F., Amoros, C., Baruah, R., Barthe, A., Berthomier, M., Bordon, S., Brockley-Blatt, C., Brysbaert, C., Capuano, G., Collier, M., Demarco, R., Fedorov, A., Ford, J., Fortunato, V., Fratter, I., Galvin, A.B., Hancock, B., Heirtzler, D., Kataria, D., Kistler, L., Lepri, S.T., Lewis, G., Loeffler, C., Marty, W., Mathon, R., Mayall, A., Mele, G., Ogasawara, K., Orlandi, M., Pacros, A., Penou, E., Persyn, S., Petiot, M., Phillips, M., Prech, L., Raines, J.M., Reden, M., Rouillard, A.P., Rousseau, A., Rubiella, J., Seran, H., Spencer, A., Thomas, J.W., Trevino, J., Verscharen, D., Wurz, P., Alapide, A., Amoruso, L., André, N., Anekallu, C., Arciuli, V., Arnett, K.L., Ascolese, R., Bancroft, C., Bland, P., Brysch, M., Calvanese, R., Castronuovo, M., ÄŒErmák, I., Chornay, D., Clemens, S., Coker, J., Collinson, G., D'Amicis, R., Dandouras, I., Darnley, R., Davies, D., Davison, G., De Los Santos, A., Devoto, P., Dirks, G., Edlund, E., Fazakerley, A., Ferris, M., Frost, C., Fruit, G., Garat, C., Génot, V., Gibson, W., Gilbert, J.A., De Giosa, V., Gradone, S., Hailey, M., Horbury, T.S., Hunt, T., Jacquey, C., Johnson, M., Lavraud, B., Lawrenson, A., Leblanc, F., Lockhart, W., Maksimovic, M., Malpus, A., Marcucci, F. et al. (2020). The Solar Orbiter Solar Wind Analyser (SWA) suite. Astronomy and Astrophysics,. doi:10.1051/0004-6361/201937259.

de Pater, I., Lissauer, J.J., 2010. Planetary Sciences. https://doi.org/10.1017/cbo9780511780561.

Piccialli, A., Montmessin, F., Belyaev, D., Mahieux, A., Fedorova, A., Marcq, E., Bertaux, J.L., Tellmann, S., Vandaele, A.C., Korablev, O., 2015. Thermal structure of Venus nightside upper atmosphere measured by stellar occultations with SPICAV/Venus Express. Planet. Space Sci. https://doi.org/10.1016/j.pss.2014.12.009.

Rampelotto, P.H. (2010). Resistance of microorganisms to extreme environmental conditions and its contribution to astrobiology. doi:10.3390/su2061602.

Saito, Y., Sauvaud, J.A., Hirahara, M., Barabash, S., Delcourt, D., Takashima, T., Asamura, K., 2010. Scientific objectives and instrumentation of Mercury Plasma Particle Experiment (MPPE) onboard MMO. Planet. Space Sci. https://doi.org/10.1016/j.pss.2008.06.003.

Seager, S., Petkowski, J.J., Gao, P., Bains, W., Bryan, N.C., Ranjan, S., Greaves, J., 2020. The Venusian Lower Atmosphere Haze as a Depot for Desiccated Microbial Life: A Proposed Life Cycle for Persistence of the Venusian Aerial Biosphere. Astrobiology. https://doi.org/10.1089/ast.2020.2244.

Shalygin, E.V., Markiewicz, W.J., Basilevsky, A.T., Titov, D.V., Ignatiev, N.I., Head, J.W., 2015. Active volcanism on Venus in the Ganiki Chasma rift zone. Geophys. Res. Lett. https://doi.org/10.1002/2015GL064088.

Sánchez Pérez, J.M., & Varga, G.I. (2018). Solar Orbiter: Consolidated report on mission analysis, SOL-ESC-RP-05500.

Snellen, I.A.G., Guzman-Ramirez, L., Hogerheijde, M.R., Hygate, A.P. S., van der Tak, F.F.S., 2020. Re-analysis of the 267 GHz ALMA observations of Venus. Astronomy & Astrophysics. https://doi.org/10.1051/0004-6361/202039717.

Steiger, C., Montagnon, E., Accomazzo, A., Ferri, P., 2020. BepiColombo mission to Mercury: First year of flight. Acta Astronaut. https://doi.org/10.1016/j.actaastro.2020.01.041.

Svedhem, H., Titov, D., Taylor, F., & Witasse, O. (2009). Venus express mission. Journal of Geophysical Research E: Planets, doi:10.1029/2008JE003290.

Titov, D.V., Ignatiev, N.I., McGouldrick, K., Wilquet, V., Wilson, C.F., 2018. Clouds and Hazes of Venus. https://doi.org/10.1007/s11214-018-0552-z.

Villanueva, G., Cordiner, M., Irwin, P., de Pater, I., Butler, B., Gurwell, M., Milam, S., Nixon, C., Luszcz-Cook, S., Wilson, C., Kofman, V., Liuzzi, G., Faggi, S., Fauchez, T., Lippi, M., Cosentino, R., Thelen, A., Moullet, A., Hartogh, P., Molter, E., Charnley, S., Arney, G., Mandell, A., Biver, N., Vandaele, A., de Kleer, K., & Kopparapu, R. (2020). No phosphine in the atmosphere of venus. arXiv:2010.14305.

von Zahn, U., Kumar, S., Niemann, H., & Prinn, R. (1983). Composition of the Venus atmosphere. In Venus (p. 299).

Vorburger, A., Wurz, P., Lammer, H., Barabash, S., Mousis, O., 2015. Monte-Carlo simulation of Callisto's exosphere. Icarus. https://doi.org/10.1016/j.icarus.2015.07.035.

Williams, D. (2016). Venus fact sheet. https://nssdc.gsfc.nasa.gov/planetary/factsheet/venusfact.html.

Wurz, P. (2005). Solar wind composition. In European Space Agency, (Special Publication) ESA SP. doi:10.1888/0333750888/2303.

Wurz, P., Abplanalp, D., Tulej, M., Lammer, H., 2012. A neutral gas mass spectrometer for the investigation of lunar volatiles. Planet. Space Sci. https://doi.org/10.1016/j.pss.2012.05.016.

Wurz, P., Lammer, H., 2003. Monte-Carlo simulation of Mercury's exosphere. Icarus. https://doi.org/10.1016/S0019-1035(03)00123-4.

Wurz, P., Rohner, U., Whitby, J.A., Kolb, C., Lammer, H., Dobnikar, P., Martín-Fernández, J.A., 2007. The lunar exosphere: The sputtering contribution. Icarus. https://doi.org/10.1016/j.icarus.2007.04.034.